

Critical Drying of Liquids

Robert Evans,¹ Maria C. Stewart,¹ and Nigel B. Wilding²

¹*H. H. Wills Physics Laboratory, University of Bristol, Royal Fort, Bristol BS8 1TL, United Kingdom*

²*Department of Physics, University of Bath, Bath BA2 7AY, United Kingdom*

(Received 19 July 2016; published 21 October 2016)

We report a detailed simulation and classical density functional theory study of the drying transition in a realistic model fluid at a smooth substrate. This transition (in which the contact angle $\theta \rightarrow 180^\circ$) is shown to be critical for both short-ranged and long-ranged substrate-fluid interaction potentials. In the latter case critical drying occurs at exactly zero attractive substrate strength. This observation permits the accurate elucidation of the character of the transition via a finite-size scaling analysis of the density probability function. We find that the critical exponent ν_{\parallel} that controls the parallel correlation length, i.e., the extent of vapor bubbles at the wall, is over twice as large as predicted by mean field and renormalization group calculations. We suggest a reason for the discrepancy. Our findings shed new light on fluctuation phenomena in fluids near hydrophobic and solvophobic interfaces.

DOI: [10.1103/PhysRevLett.117.176102](https://doi.org/10.1103/PhysRevLett.117.176102)

With new types of nanostructured hydrophobic substrates and coatings finding application in systems such as microfluidic devices, self-cleaning surfaces, and chemical separation processes, there is considerable interdisciplinary interest in the behavior of fluids in contact with weakly attractive surfaces [1–4]. Thermodynamically, the state of a liquid drop near a solid substrate (or “wall”) is characterized by the contact angle θ that the drop makes with the surface. The weaker the wall-fluid attraction, the larger θ becomes. In the limit $\theta \rightarrow 180^\circ$ a fluid at vapor-liquid coexistence undergoes a surface phase transition known as *drying* whereby a macroscopic film of vapor (v) intrudes between the wall (w) and the bulk liquid (l); this is the analogue of the well-known wetting transition that occurs for strongly attractive surfaces as $\theta \rightarrow 0$. Wetting has been studied in detail; see [5] for a review and [6] for a recent investigation of water. Theory and simulation has often focused on Ising models, e.g. [7–9], whose special symmetry implies that wetting and drying are equivalent. However in real fluids, wetting and drying are distinct phenomena and very little is known concerning the fundamental properties of either transition. Previous work has led to long-standing controversies, in particular, as to whether the drying transition in model fluids is first order or continuous (critical) [10–16], or even whether it exists at all [17,18]. Accordingly there is a need for clear elucidation of the nature of the approach to drying in fluids, not just in thermodynamic terms but also with regard to the local density fluctuations that characterize the transition.

The main barriers to computational progress in tackling drying in realistic fluids has been the dearth of techniques for locating surface phase transitions accurately, combined with the lack of rigorous measures for quantifying their key characteristics. In this Letter we deploy state-of-the-art Monte Carlo simulation techniques and classical density

functional theory (DFT) together with a rigorously defined measure of the local compressibility to study a realistic model fluid near an attractive structureless wall. We begin by settling the long-standing controversy concerning the order of the drying transition: For the (truncated) Lennard-Jones (LJ) fluid that we consider, drying is continuous. This is true for both a short-ranged (SR) and a long-ranged (LR) van der Waals wall-fluid interaction potential—a finding that contrasts with wetting in the same system which is a discontinuous transition for the LR wall-fluid potential but continuous for the SR case. Moreover, we show that for LR wall-fluid potentials, drying occurs at *zero* attractive wall strength. This represents the first instance of a surface phase transition in 3d whose parameters are exactly known and thus provides an opportunity to study a surface critical point free from uncertainty regarding its location (a problem that has previously plagued Ising model studies of critical wetting [9]). By performing a finite size scaling (FSS) analysis of the density fluctuations that characterize the near critical region in the LR case, we demonstrate that critical drying in simulations is associated with a *single* divergent correlation length ξ_{\parallel} , that for density correlations parallel to the wall. The interfacial roughness ξ_{\perp} , arising from capillary wave fluctuations, is heavily dampened by finite-size effects to a magnitude of order the particle diameter and plays no role in the FSS. Our analysis allows us to estimate the effective critical exponent ν_{\parallel} describing the growth of ξ_{\parallel} . We note that our 3d system is at the upper critical dimension and, in contrast to the case of SR wall-fluid interactions, a renormalization group (RG) analysis indicates [19] that the critical exponents should take their mean-field values. However, our simulation estimate of ν_{\parallel} is much larger than that predicted by mean-field and furthermore appears to be temperature dependent.

The model we consider is a LJ fluid in a slit pore composed of a pair of structureless parallel walls of area L^2 separated by a distance D ; periodic boundary conditions apply in the directions parallel to the walls. Fluid-fluid interactions are truncated at $r_c = 2.5\sigma$, where σ is the LJ diameter, and particles interact with each wall via a wall-fluid potential $W(z)$, with z the perpendicular particle-wall distance. We consider two forms for $W(z)$ commonly encountered in the adsorption literature: (i) the SR case of a hard wall plus square well potential of range 0.5σ , and, (ii) the LR case of a hard wall plus a nontruncated long-ranged attraction decaying as z^{-3} . Both wall-fluid potentials are parametrized in terms of the well depth ϵ . To study these systems we deploy grand canonical Monte Carlo (GCMC) simulation and classical DFT. The latter approximates the repulsive LJ core as a hard core, whose free energy is treated via fundamental measure theory, while the attractive part of the LJ potential is treated in a mean field fashion [19,22,23]. The GCMC simulations impose the temperature T , chemical potential μ , and the depth ϵ of $W(z)$, which we quote in units of $k_B T$. Flat histogram techniques [24] were used to record the local number density profile $\rho(z)$ and the overall number density ρ . All results were accumulated at liquid-vapor coexistence for two subcritical temperatures $T = 0.775T_c$ and $T = 0.842T_c$, with T_c the bulk critical temperature known from previous work [25]. The coexistence value of μ was determined to high precision for a large fully periodic system using recently developed bespoke techniques [26] which ameliorate the sampling problems at low T and large volumes that arise from “droplet” transitions [27].

The dependence of the contact angle on the wall-fluid well depth ϵ was estimated for both the SR and LR wall-fluid potentials via direct measurements of the interfacial tensions appearing in Young’s equation, $\gamma_{lv} \cos(\theta) = \gamma_{wv} - \gamma_{wl}$, using a method detailed elsewhere [28,29]. The results are shown in Fig. 1 and span the range from wetting [$\cos(\theta) = 1$] to drying [$\cos(\theta) = -1$]. Interestingly the two forms of wall-fluid potential show distinct behavior. For the SR case, both wetting and drying are continuous for this range of $W(z)$: $\cos(\theta)$ approaches the respective limits tangentially [30]. For the LR case, the same is true for drying, but wetting is first order: $\cos(\theta)$ approaches unity with a nonzero linear slope. The DFT results in Fig. 1 display the same transitions as in simulation.

In what follows we focus on drying in the LR case which is the situation most commonly studied in simulations of LJ fluids [31–33] and of models of water [34–36]. From Fig. 1 it appears at first sight that simulations indicate that drying occurs at a nonzero (albeit small) value of ϵ . However, while measurements of $\cos(\theta)$ are reliable indicators of the order of the transitions, they fail to provide accurate estimates for the critical well depth ϵ_c . The problem goes well beyond that of the inherent difficulty of determining the point at which $\cos(\theta) = -1$ when the approach to this

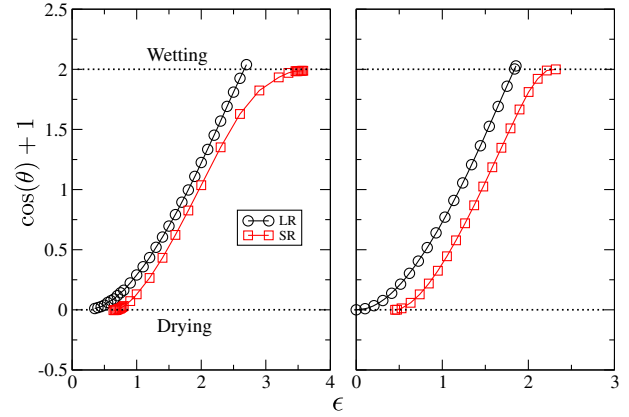


FIG. 1. Left: GCMC results for $\cos(\theta) + 1$ versus ϵ for the SR and LR wall potential at $T = 0.775T_c$, for $L = 15\sigma$, $D = 30\sigma$. For the LR case a FSS analysis of the GCMC data yields critical drying at $\epsilon_c = 0$, as predicted by theory while for the SR case a FSS analysis gives critical drying at $\epsilon_c = 0.52(2)$ and critical wetting at $\epsilon_c = 4.25(5)$. Right: corresponding DFT results.

limit is tangential. Instead the main issue is one of critical finite-size effects which systematically shift the apparent critical point with respect to its true value. Accordingly a FSS analysis of the near-critical fluctuations is vital for determining accurately the drying point.

Our approach is to examine the probability distribution function of the number density $p(\rho)$, and specifically its dependence on ϵ and the wall dimension L . Results are shown in Fig. 2 and reveal that for sufficiently large ϵ and L , $p(\rho)$ exhibits a peak at high density. In the absence of finite-size effects, this peak corresponds to the liquid phase in contact with the wall and is a signature of partial drying, i.e., $\theta < 180^\circ$. However, the situation is more subtle. On decreasing ϵ , the peak in $p(\rho)$ disappears into a plateau. On further

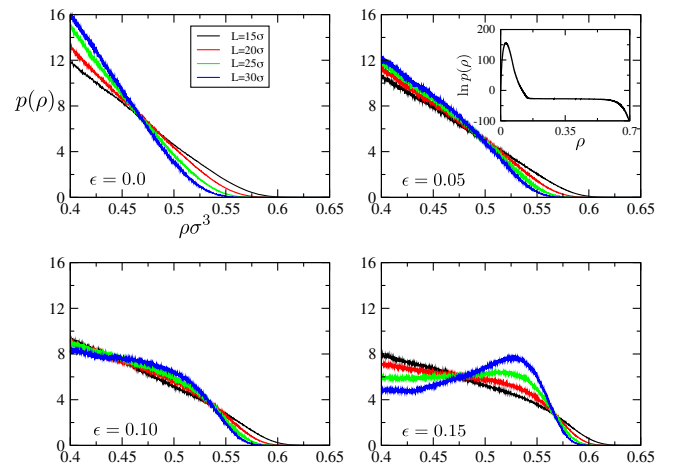


FIG. 2. GCMC results for $p(\rho)$ for the LR wall potential for $D = 30\sigma$ and various L at a selection of near-critical values of ϵ . Note that at small ρ capillary evaporation occurs, manifest as a vaporlike peak in $p(\rho)$ as shown in the inset for $\epsilon = 0.05$, $L = 15\sigma$.

reducing ϵ , $p(\rho)$ becomes monotonically decreasing with a bulge which gradually diminishes until, at $\epsilon = 0$, the distribution comprises a linear part and a tail. The range of values of ϵ over which this scenario plays out decreases with increasing L . Only for $\epsilon = 0$ is the form of $p(\rho)$ scale invariant, i.e., no peak begins to form as L is increased. Consequently this wall strength marks the critical drying point. Significantly, both DFT (cf. Fig. 1) and binding potential calculations [19] also predict critical drying for $\epsilon = 0$. Note for $\epsilon = 0$, $W(z)$ reduces to the hard wall potential and complete drying occurs for all $T < T_c$. What is remarkable is that the transition is critical and occurs precisely at $\epsilon = 0$ for all $W(z)$ exhibiting power-law decay [19].

The fact that for a LR wall potential drying is critical with $\epsilon_c = 0$ is confirmed by measurements of the compressibility profile $\chi(z) \equiv \partial\rho(z)/\partial\mu$. This quantity was introduced previously [37,38] and has subsequently proven a sensitive measure of the link between the contact angle θ and the local structure near hydrophobic or solvophobic surfaces [23,29]. Its form probes the transverse density-density correlation function and thus the correlation length ξ_{\parallel} . GCMC measurements of the maximum of $\chi(z)$ are shown in Fig. 3 and demonstrate a power law divergence as ϵ is reduced to zero, implying that ξ_{\parallel} diverges at this wall strength. This divergence is confirmed by DFT measurements of $\chi(z)$ as shown in the inset.

The form of $p(\rho)$ at $\epsilon = 0$ (Fig. 2), corresponding to a hard wall, represents a hallmark of critical drying and yields fundamental insight concerning its character. It comprises a linearly sloped part at lower density plus a

tail at higher densities. With increasing L , the tail density shifts to lower values. Interestingly, the form and L dependence of $p(\rho|\epsilon_c)$ cannot be rationalized in terms of a FSS ansatz previously proposed for critical wetting in 3d Ising models [8,9]. That theory presumes the critical divergence of not just ξ_{\parallel} but also of the perpendicular correlation length ξ_{\perp} which measures the roughness of the emerging liquid-vapor interface due to capillary fluctuations. While our measurements of $\chi(z)$ provide ample evidence for a divergent ξ_{\parallel} , we find no signs that ξ_{\perp} is large in our simulations. This is because of the extremely strong finite-size dampening of the surface roughness for $d = 3$. General capillary wave arguments, e.g. [22,30,39], for a single unbinding vapor-liquid interface predict that $\xi_{\perp} \approx \sqrt{(k_B T / 2\pi\gamma_{lv}) \ln(L/\xi_b)}$. Thus the interfacial roughness depends on the finite lateral dimension of the system. Given the strength of this dampening, one cannot expect ξ_{\perp} to become large on the scale of the particle diameter (or indeed the bulk correlation length ξ_b) for currently accessible simulation sizes.

These observations, together with the results of Figs. 2 and 3, imply the following picture for critical drying in simulations of 3d systems. As $\epsilon \rightarrow \epsilon_c^+$, bubbles of vapor form at the wall whose lateral size corresponds to $\xi_{\parallel} \sim (\epsilon - \epsilon_c)^{-\nu_{\parallel}}$ (cf. the snapshot in Fig. 4 and the movie in the Supplemental Material [19]) but whose perpendicular length scale remains microscopic. As ξ_{\parallel} approaches L , the liquid unbinds from the wall to form a “slab,” surrounded by vapor. Essentially this process can be viewed as premature drying induced by the finite system size. The slab surface is rather sharp and localized due to the

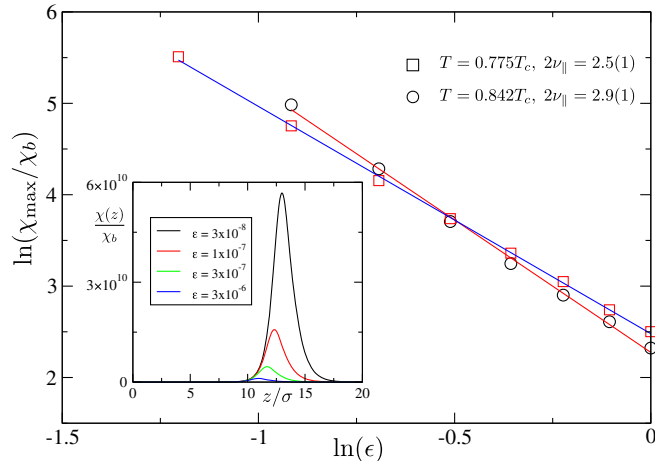


FIG. 3. GCMC measurements of the scaling of the peak in $\chi(z)/\chi_b$ with wall-fluid potential well depth ϵ for the LR wall-fluid potential. χ_b is the bulk liquid phase compressibility. The system size is $L = 50\sigma$, $D = 30\sigma$. Inset: DFT results for $\chi(z)/\chi_b$ for a single wall, showing the divergence as $\epsilon \rightarrow 0$. This occurs in the way binding potential arguments predict, i.e., $\ln(\chi(l)) \sim l$ with l the drying layer thickness and $\chi(l) \sim \xi_{\parallel}^2$; see Fig. S1 of [19].

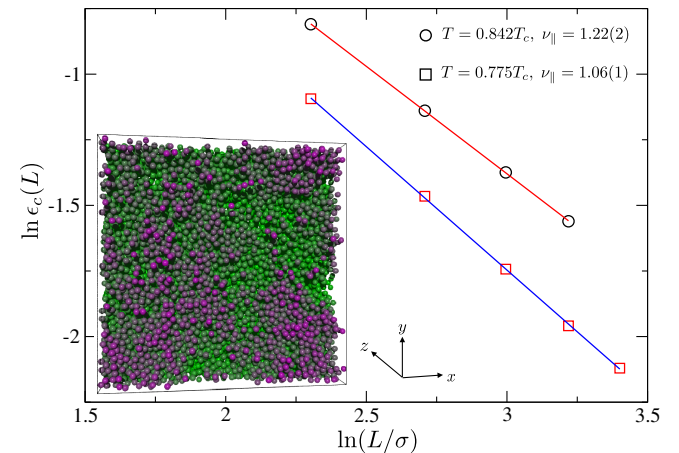


FIG. 4. The scaling of $\epsilon_c(L)$, i.e., the wall strength at which a peak appears in $p(\rho)$, as a function of L for the LR wall-fluid potential. Data are shown for two subcritical temperatures. Inset: simulation snapshot for a system with $L = 40\sigma$, $\epsilon = 0.2$. Particles are color coded according to their distance from the wall at $z = 0$. A large correlation length is manifest in the vapor close to the wall; see the Supplemental Material [19].

dampening of interfacial roughness and the slab thickness (in the z direction) is therefore proportional to ρ . Accordingly, the linear decrease of $p(\rho|\epsilon = 0)$ seen at low to moderate densities in Fig. 2 arises simply from the “entropic repulsion” of the slab and the wall: the number of positions for the slab center along the z axis that are allowed by the presence of the wall varies linearly with slab thickness. The high density tail of $p(\rho)$ on the other hand reflects the free energy cost of pushing the liquid up against the wall, the act of which quenches the parallel density fluctuations. Its L dependence arises—as shown in the Supplemental Material [19]—from a constant repulsive pressure on the liquid-vapor interface by the wall, giving rise to a force which scales simply with the wall area L^2 .

Neither the fluctuation in the thickness of the unbound liquid slab occurring at low-moderate densities nor the high density tail is directly associated with criticality, and thus one cannot expect $p(\rho)$ to exhibit nontrivial FSS behavior as a whole. Rather, the signature of near critical fluctuations is manifest in the density range where the liquid is still (weakly) bound to the wall but exhibits strong parallel density fluctuations. This corresponds to the liquid peak in Fig. 2, the height of which depends on ξ_{\parallel} and vanishes when $\xi_{\parallel} \approx L$ allowing the liquid slab to unbind from the wall. Simple FSS dictates that this vanishing occurs not at ϵ_c but at the larger effective value $\epsilon_c(L) = \epsilon_c + aL^{-1/\nu_{\parallel}}$ (which corresponds also to the wall strength at which the surface tension measurements with Young’s equation predict $\theta = 180^\circ$). The critical wall strength ϵ_c can differ substantially from $\epsilon_c(L)$ and is determined most accurately as the largest value of ϵ for which $p(\rho)$ assumes an L -independent form. However, in contrast to the rich structure of the density distribution at bulk criticality [25] the novel feature of critical drying is the surprising simplicity of $p(\rho|\epsilon_c)$.

We have determined the value of ν_{\parallel} via the anticipated FSS $\epsilon_c(L) \sim L^{-1/\nu_{\parallel}}$, $\epsilon_c = 0$ for the LR case. For a number of choices of L we measured $\epsilon_c(L)$ accurately (using histogram extrapolation techniques) from the vanishing of the liquid peak of $p(\rho)$ (cf. Fig. 2). As Fig. 4 shows, we do indeed see power law scaling, from which we can extract an estimate of ν_{\parallel} . Interestingly, however, this estimate exceeds the prediction $\nu_{\parallel} = 0.5$ of mean field and RG theories (see the Supplemental Material [19]) by over a factor of 2 and additionally appears to show a clear temperature dependence. This discrepancy with theory is further mirrored in the behavior of $\chi(z)$ (Fig. 3) for which one expects [19] that $\chi_{\max} \sim (\epsilon - \epsilon_c)^{-2\nu_{\parallel}}$. Here too the simulation estimates of ν_{\parallel} are over twice the theoretical prediction and show a clear temperature dependence.

We summarize and discuss our findings. A realistic model liquid in contact with a substrate that exerts a long-ranged van der Waals attraction undergoes a critical drying transition at zero attractive wall strength. From the general theory [19], we can infer that the same transition, at $\epsilon = 0$,

should occur for models of water at such walls. Indeed the occurrence of critical drying would account for recent results [34–36,40] displaying very large contact angles and enhanced fluctuations in simulations of water at strongly hydrophobic LR substrates.

Analysis of density fluctuations provides fresh insight into the nature of critical drying, revealing that (in simulations at least) there is only one divergent correlation length, ξ_{\parallel} , associated with the growth of vapor bubbles at the wall. Of course capillary wave theory predicts that ξ_{\perp} diverges for a free interface in the absence of gravity, or at an infinite single wall in the limit of wetting or drying, but it seems one cannot observe a macroscopically large ξ_{\perp} in fluid simulations, which therefore miss a key element of the theoretical picture [41]. It is tempting to speculate that a single diverging ξ_{\parallel} could imply that critical drying in simulations is effectively controlled by the 2D Ising fixed point for which $\nu = 1$. This value is indeed much closer to our estimate of ν_{\parallel} than the predictions of RG theory for the LR case. Clearly further work is required to address these subtle but important issues.

Our methods for locating and characterizing critical drying should prove useful for elucidating critical wetting transitions in $d = 3$. Here fundamental questions remain regarding the relationship between simulation results and theoretical predictions [8,9,42–44]. In Fig. 1 our results for $\cos(\theta)$ for a SR (square-well) wall indicate critical wetting. Preliminary investigations [45] of this system reveal closely analogous phenomenology to that seen at drying, namely a vapor peak in $p(\rho)$ which gradually disappears on increasing ϵ until, at the wetting point, $p(\rho)$ assumes a scale invariant form comprising a low density tail and a linear part extending to high density. The implication is that like critical drying, critical wetting in simulations will occur in the absence of a large ξ_{\perp} .

Our findings settle the long-standing controversy regarding the order of the drying transition [10–16]. Furthermore they help explain the original misconception. This arose, we believe, because for fluids in a slit pore the liquid phase is metastable with respect to capillary evaporation (cf. the vapor peak in the inset of Fig. 2). As $\epsilon \rightarrow \epsilon_c(L)^+$, the liquid unbinds from the wall and the liquid-vapor interface wanders towards the slit center where it annihilates with its counterpart from the other wall to form a pure vapor phase. In the absence of the insights provided by the present work, it is easy to mistake this discontinuous evaporation for the critical surface phase transition that precipitates it [10–12]. Note, however, that since the results of Fig. 2 focus on the regime of moderate to large ρ they are unaffected by evaporation [46].

Finally, as regards the experimental relevance of our findings, the observation that the drying transition in liquids is critical irrespective of the range of the wall-fluid interactions, should prove important when interpreting observations of the properties of fluids near hydro- or

solvophobic interfaces, in which there is growing technological [1–3] and fundamental [47,48] interest. We do not expect the basic phenomenology of critical drying to be altered if one considers a substrate corrugated on the atomic scale rather than a planar one. It remains to be seen to what extent the phenomenology applies for nanostructured surfaces with larger characteristic periods. Although real hydrophobic surfaces never quite attain contact angles $\theta = 180^\circ$, the effects of criticality should extend over a wide range of $\theta < 180^\circ$ [23,29] and experiments such as those of Ref. [49] might be able to confirm the existence of enhanced density fluctuations in the vicinity of a hydrophobic substrate.

R. E. acknowledges Leverhulme Trust for the award of a Fellowship No. EM-2016-031.

-
- [1] J. T. Simpson, S. R. Hunter, and T. Aytug, *Rep. Prog. Phys.* **78**, 086501 (2015).
- [2] X.-M. Li, D. Reinhoudt, and M. Crego-Calama, *Chem. Soc. Rev.* **36**, 1350 (2007).
- [3] E. Ueda and P. A. Levkin, *Adv. Mater.* **25**, 1234 (2013).
- [4] A. Checco, B. M. Ocko, A. Rahman, C. T. Black, M. Tasinkevych, A. Giacomello, and S. Dietrich, *Phys. Rev. Lett.* **112**, 216101 (2014).
- [5] D. Bonn, J. Eggers, J. Indekeu, J. Meunier, and E. Rolley, *Rev. Mod. Phys.* **81**, 739 (2009).
- [6] S. R. Friedman, M. Khalil, and P. Taborek, *Phys. Rev. Lett.* **111**, 226101 (2013).
- [7] K. Binder, D. P. Landau, and S. Wansleben, *Phys. Rev. B* **40**, 6971 (1989).
- [8] E. V. Albano and K. Binder, *Phys. Rev. Lett.* **109**, 036101 (2012).
- [9] P. Bryk and K. Binder, *Phys. Rev. E* **88**, 030401 (2013).
- [10] F. van Swol and J. R. Henderson, *Phys. Rev. A* **40**, 2567 (1989).
- [11] J. R. Henderson and F. van Swol, *J. Phys. Condens. Matter* **2**, 4537 (1990).
- [12] F. van Swol and J. R. Henderson, *Phys. Rev. A* **43**, 2932 (1991).
- [13] M. J. P. Nijmeijer, C. Bruin, A. F. Bakker, and J. M. J. van Leeuwen, *J. Phys. Condens. Matter* **4**, 15 (1992).
- [14] M. J. P. Nijmeijer, C. Bruin, A. F. Bakker, and J. M. J. van Leeuwen, *Phys. Rev. B* **44**, 834 (1991).
- [15] J. R. Henderson, P. Tarazona, F. van Swol, and E. Velasco, *J. Chem. Phys.* **96**, 4633 (1992).
- [16] C. Bruin, M. J. P. Nijmeijer, and R. M. Crevecoeur, *J. Chem. Phys.* **102**, 7622 (1995).
- [17] F. Ancilotto, S. Curtarolo, F. Toigo, and M. W. Cole, *Phys. Rev. Lett.* **87**, 206103 (2001).
- [18] A. Oleinikova, I. Brovchenko, and A. Geiger, *J. Phys. Condens. Matter* **17**, 7845 (2005).
- [19] See Supplemental Material at <http://link.aps.org/supplemental/10.1103/PhysRevLett.117.176102>, which includes [20,21], for (a) details of binding potential calculations; (b) details of DFT calculation; (c) details of how the tails of $p(\rho)$ scale with the wall dimension L ; and (d) a movie of the near critical interface.
- [20] M. P. Nightingale, W. F. Saam, and M. Schick, *Phys. Rev. Lett.* **51**, 1275 (1983).
- [21] E. Brézin, B. I. Halperin, and S. Leibler, *Phys. Rev. Lett.* **50**, 1387 (1983).
- [22] R. Evans, in *Fundamentals of Inhomogeneous Fluids*, edited by D. Henderson (Dekker, New York, 1992), p. 85.
- [23] R. Evans and M. C. Stewart, *J. Phys. Condens. Matter* **27**, 194111 (2015).
- [24] B. A. Berg and T. Neuhaus, *Phys. Rev. Lett.* **68**, 9 (1992).
- [25] N. B. Wilding, *Phys. Rev. E* **52**, 602 (1995).
- [26] N. B. Wilding, *J. Phys. Condens. Matter* **28**, 414016 (2016).
- [27] L. G. MacDowell, P. Virnau, M. Müller, and K. Binder, *J. Chem. Phys.* **120**, 5293 (2004).
- [28] M. Müller and L. G. MacDowell, *Macromolecules* **33**, 3902 (2000).
- [29] R. Evans and N. B. Wilding, *Phys. Rev. Lett.* **115**, 016103 (2015).
- [30] S. Dietrich, *Phase Transitions and Critical Phenomena*, edited by C. Domb and J. L. Lebowitz (Academic, London, 1988), Vol. 12, p. 1.
- [31] Y. Fan and P. A. Monson, *J. Chem. Phys.* **99**, 6897 (1993).
- [32] P. Bryk, S. Sokołowski, and D. Henderson, *J. Chem. Phys.* **110**, 15 (1999).
- [33] K. S. Rane, V. Kumar, and J. R. Errington, *J. Chem. Phys.* **135**, 234102 (2011).
- [34] V. Kumar and J. R. Errington, *Mol. Simul.* **39**, 1143 (2013).
- [35] V. Kumar and J. R. Errington, *J. Phys. Chem. C* **117**, 23017 (2013).
- [36] A. P. Willard and D. Chandler, *J. Chem. Phys.* **141**, 18C519 (2014).
- [37] P. Tarazona and R. Evans, *Mol. Phys.* **47**, 1033 (1982).
- [38] R. Evans and A. O. Parry, *J. Phys. Condens. Matter* **2**, SA15 (1990).
- [39] M. P. Gelfand and M. E. Fisher, *Physica (Amsterdam)* **166A**, 1 (1990).
- [40] R. Godawat, S. Jamadagni, V. Venkateshwara, and S. Garde, [arXiv:1409.2570](https://arxiv.org/abs/1409.2570).
- [41] One should also note that, in simulation, the maximum thickness of the drying (vapor) layer that can be investigated is only a few particle diameters.
- [42] A. O. Parry, C. Rascón, N. R. Bernardino, and J. M. Romero-Enrique, *Phys. Rev. Lett.* **100**, 136105 (2008).
- [43] A. O. Parry, C. Rascón, N. R. Bernardino, and J. M. Romero-Enrique, *J. Phys. Condens. Matter* **20**, 494234 (2008).
- [44] A. O. Parry and C. Rascón, *J. Low Temp. Phys.* **157**, 149 (2009).
- [45] R. Evans, M. C. Stewart, and N. B. Wilding (unpublished).
- [46] In a semi-infinite system, there is only a single vapor-liquid interface, which can wander arbitrarily far from the wall and the evaporation transition does not exist.
- [47] M. Mezger, H. Reichert, B. M. Ocko, J. Daillant, and H. Dosch, *Phys. Rev. Lett.* **107**, 249801 (2011).
- [48] A. Uysal, M. Chu, B. Stripe, A. Timalisina, S. Chattopadhyay, C. M. Schlepütz, T. J. Marks, and P. Dutta, *Phys. Rev. B* **88**, 035431 (2013).
- [49] K. Nygård, S. Sarman, K. Hyltegren, S. Chodankar, E. Perret, J. Buitenhuis, J. F. van der Veen, and R. Kjellander, *Phys. Rev. X* **6**, 011014 (2016).